Hokkaido Mathematical Journal Vol. 36 (2007) p. 891–918

Analysis of conforming and nonconforming quadrilateral finite element methods for the Helmholtz equation

Taeyoung Ha, Ki-tak Lee and Dongwoo Sheen

(Received May 6, 2007; Revised August 8, 2007)

Abstract. In this paper we analyze numerical dispersion relation of some conforming and nonconforming quadrilateral finite elements. The elements employed in this analysis are the standard Q_1 conforming finite element, the DSSY nonconforming element [5] and the P_1-nonconforming quadrilateral finite element [14]. Several aspects of comparative analyses of the above three elements for two or three dimensional problems are shown.

Key words: dispersion relation, Helmholtz equation, finite elements.

1. Introduction

The Helmholtz equation $-(\omega^2/c^2)u - \Delta u = 0$ in a domain Ω may be either an eigenvalue problem or a uniquely solvable problem, depending on the boundary condition on the boundary $\partial\Omega$. Indeed, under the classical Dirichlet or Neumann boundary condition, an integration by parts of the $L^2(\Omega)$ inner-product yields that there exists an eigensolution u associated with the angular eigenfrequency ω such that $\omega^2 = \int_\Omega |\nabla u|^2 dx / \int_\Omega |u/c|^2 dx$. However, if the boundary condition is replaced by an absorbing boundary condition of the type $i(\omega/c)u + \partial u/\partial\nu = 0$, the problem turns out to be a uniquely solvable problem for all $\omega \neq 0$ ([4]). The latter case supports an interesting idea to solve the time-domain wave equation in the frequency-space formulation in massively parallel computer using a different process for different non-zero frequency. Such a direction was introduced by Douglas-Santos-Sheen-Bennethum in [4]; also in the same paper a first rigorous finite element error analysis was carried out for the one-dimensional Helmholtz problem. The $L^2(\Omega)$ and $H^1(\Omega)$ finite element error estimates turn out to depend essentially the multiplication of the frequency and the mesh size.

Later, Babuška and Ihlenburg [12], and their colleges, looked deeply into this dependence and raised an important issue, what is called the "pollution effect". The discrete solutions using the standard Galerkin finite element method results in inaccurate solutions if the mesh size is not sufficiently

2000 Mathematics Subject Classification : Primary 81U30; Secondary 35J05.

small compared to the size of wave number [1, 12, 11, 10, 4, 3]. Numerical dispersion seems to be a major source for the pollution effect. Therefore, unless the size of wave number k is sufficiently small, some kind of specific finite element techniques, such as hp methods, need to be employed. See also extensive surveys on numerical methods for Helmholtz problems [8, 16].

In this paper we will examine the dispersion effects in solving Helmholtz problems by the finite element method using quadrilateral or rectangular elements of lowest order. Specifically, the following three conforming and nonconforming element methods will be analyzed: (1) the standard Q_1 conforming element (abbreviated as the "Q_1 element"); (2) the DSSY nonconforming element introduced by Douglas *et al.* [5] (abbreviated as the "DSSY NC" element, or the "DSSY" element) which is a modified rotated Q_1 element of Rannacher and Turek [15]; and (3) the P_1-nonconforming quadrilateral(hexahedron) element [14] (abbreviated as the " P_1-NC element"). Santos *et al.* [20] and Zyserman *et al.* [19] gave detailed dispersion analyses for solving the Helmholtz equation, and elastic and viscoelastic equations by comparing between the Q_1 conforming and the DSSY NC finite element methods. It is shown in [1, 20, 19] that the L^2-error of the DSSY NC element behaves better in reducing numerical dispersion than that of Q_1 element based on the same size of grids. However, it has been questionable if the DSSY NC element is actually cheaper than the Q_1 conforming element to achieve desired accuracy. One of the purposes of the our paper is to investigate the actual costs of computation to reduce errors up to certain tolerance instead of estimating errors based on the size of meshes. In the numerical experiments we concentrate on the number of elements and the degrees of freedom necessary to guarantee the L^2 and broken H^1 errors which are smaller than given tolerance ϵ. Our results imply that the P_1-NC quadrilateral element requires the least degrees of freedom among the three elements.

The organization of this paper is as follows. In Section 2, the dispersion relation and model problem are stated. In Section 3 a brief review of the P_1-NC quadrilateral element [14] is also given together its weak formulation. In Section 4, numerical dispersion relations are shown for two and three dimensional problems when the P_1-NC quadrilateral elements are employed. In Section 5, we analyze the dispersion relation and investigate the pollution effects by comparing the three finite elements. Finally conclusions are given in Section 6.

2. Dispersion relation and model problem

In the approximation of wave propagation the two most annoying sources of numerical errors are numerical dissipation and dispersion. Numerical dissipations result in usually reducing or sometimes magnifying wave amplitudes. Numerical dispersions are related with phase changes of computed wave forms and thus may result in some erroneous approximation of the wave velocity [13, 17].

Consider the following wave equation

$$\frac{1}{c^2}u_{tt} - \Delta u = 0. \tag{2.1}$$

whose typical plane wave solution is given in the form

$$u(\mathbf{x},\, t) = Ae^{i\varphi(\mathbf{x},\, t)}, \tag{2.2}$$

where A, $\mathbf{k} = \nabla\varphi$ and $\omega = -\partial\varphi/\partial t$ denote the amplitude, the wave vector, and the angular frequency, with the wavelength $\lambda = 2\pi/\omega$ [18]. The phase $\varphi(\mathbf{x},\, t) = \omega t - \mathbf{k}\cdot\mathbf{x}$ determines phase surfaces $\{(\mathbf{x},\, t)\colon \varphi(\mathbf{x},\, t) = \text{constant}\}$ for each *constant*. Then the equation (2.1) with the solution (2.2) reduces to $\omega^2/c^2 - |\mathbf{k}|^2 = 0$, with which the dispersion relation, phase and group velocities are given in the form

$$\omega = \omega(\mathbf{k}) = \pm c|\mathbf{k}|, \quad \mathbf{c} = \frac{\omega(\mathbf{k})}{k}\widehat{\mathbf{k}}, \quad \mathbf{c}_g = \frac{\partial\omega(\mathbf{k})}{\partial\mathbf{k}}, \tag{2.3}$$

where $k = |\mathbf{k}|$ and $\widehat{\mathbf{k}} = \frac{1}{k}\mathbf{k}$. Since the wave equation is linear, the phase speed should not differ from the speed c of wave propagation.

Let $u_h(\mathbf{x},\, t)$ be a numerical approximate solution to (2.1). While the normalized plane wave solution $u(\mathbf{x},\, t) = e^{i(\omega t - \mathbf{k}\cdot\mathbf{x})}$ has the value $u(\mathbf{x}_{jk},\, n\Delta t)$ $= e^{i(\omega n\Delta t - \mathbf{k}\cdot\mathbf{x}_{jk})}$ at the nodal point $\mathbf{x}_{jk} = (jh,\, kh)$ at $n\Delta t$, the numerical solution u_h may have a different value with a possible amplitude change. However, the nodal values of the numerical solution will approximate the feature of wave structure with an approximate angular frequency and an approximate wave vector, denoted by ω^h and $\mathbf{k}^h$, respectively. Representing the numerical dissipative or amplifying factor by e^{σ^h} (assuming that $\sigma^h \in \mathbb{R}$), the numerical solution at the nodal point $\mathbf{x}_{jk}$ at $n\Delta t$ has the value

$$u_h(\mathbf{x}_{jk},\, n\Delta t) = e^{(\sigma^h + i\omega^h)n\Delta t - i\mathbf{k}^h\cdot\mathbf{x}_{jk}}. \tag{2.4}$$

Usually careful schemes are chosen so that $\sigma^h \equiv 0$, independent of the

numerical wave vector $\mathbf{k}^h$. With such numerical methods, the numerical dispersion relation is defined by the relation bewteen the approximate angular frequency and wave vector in the form:

$$\omega^h = \omega^h(\mathbf{k}^h), \tag{2.5}$$

with the numerical phase and group velocities given by

$$\mathbf{c}^h = \frac{\omega^h(\mathbf{k}^h)}{|\mathbf{k}^h|}\widehat{\mathbf{k}}^h, \quad \mathbf{c}_g^h = \frac{\partial\omega^h(\mathbf{k}^h)}{\partial\mathbf{k}^h}, \quad \text{with} \quad \widehat{\mathbf{k}^h} = \frac{|\mathbf{k}^h|}{\mathbf{k}^h}. \tag{2.6}$$

Let us turn to the Helmholtz equation, $-(\omega^2/c^2)\widehat{u} - \Delta\widehat{u} = 0$, which circumvents the time variable and thus it does not suffer from numerical dissipation or amplification. In this case, (2.4) is replaced by $\widehat{u}_h(\mathbf{x}_{jk}) = e^{-i\mathbf{k}^h\cdot\mathbf{x}_{jk}}$, and the ω^h's in (2.5) and (2.6) should be replaced by ω. However, its numerical solutions in the high frequency range exhibit malicious numerical errors, mainly due to numerical dispersions in the approximation of the Helmholtz equation, which will be our subject to investigate in the paper.

2.1. The Helmholtz model problem

Let Ω be a simply-connected bounded open polygonal (polyhedral) domain with an artificial boundary $\Gamma = \partial\Omega$. Assume that the origin O is contained in Ω. With the convenient first-order absorbing boundary condition (2.7b) imposed on the Γ, one then has the following Helmholtz problem:

$$-\frac{\omega^2}{c^2}u(\mathbf{x},\,\omega) - \Delta u(\mathbf{x},\,\omega) = f(\mathbf{x},\,\omega) \quad \text{in } \Omega, \tag{2.7a}$$

$$i\frac{\omega}{c}u(\mathbf{x},\,\omega) + \frac{\partial u}{\partial\nu}(\mathbf{x},\,\omega) = 0 \quad \text{on } \Gamma. \tag{2.7b}$$

Here, and in what follows, the hats $(\widehat{\ })$ on the functions u and f will be dropped to simplify notations. Denote by $L^2(\Omega)$ and $L^2(\Gamma)$ the complex Hilbert spaces of square integrable functions in Ω and Γ with the inner products $(\,\cdot\,,\,\cdot\,)$ and $\langle\,\cdot\,,\,\cdot\,\rangle_\Gamma$, respectively; the corresponding norms are denoted by $\|u\|_0 = \big[\int_\Omega |u|^2 d\mathbf{x}\big]^{1/2}$ and $|u|_{0,\Gamma} = \big[\int_{\partial\Omega} |u|^2 d\sigma(\mathbf{x})\big]^{1/2}$. The standard notations for Sobolev spaces will be used; for instance, $H^1(\Omega) = \{v \in L^2(\Omega); |\nabla v| \in L^2(\Omega)\}$. with its seminorm and norm given by $|u|_1 = \big[\int_\Omega |\nabla u|^2 d\mathbf{x}\big]^{1/2}$ and $\|u\|_1 = \big[\|u\|_0^2 + |u|_1^2\big]^{1/2}$, respectively.

The weak formulation for (2.7) is then given by finding $u \in H^1(\Omega)$ such

that

$$a(u,\, v) = F(v), \quad \forall v \in H^1(\Omega), \tag{2.8}$$

where

$$a(u,\, v) = -\Big(\frac{\omega^2}{c^2}u,\, v\Big) + (\nabla u,\, \nabla v) + i\omega \left\langle \frac{1}{c}u,\, v \right\rangle_{\Gamma};\ F(v) = (f,\, v).$$

The well-posedness of Problem (2.8) is well understood [4, 3] and elliptic regularity estimates are given in [6].

3. The nonconforming finite elements

In this section we briefly review the P_1-nonconforming element on quadrilaterals in [14].

3.1. The P_1-nonconforming element on quadrilaterals

Let Q be a (convex) quadrilateral with the vertices v_j and the midpoints m_j of edges, such that $m_j = (v_{j-1}+v_j)/2$, $1 \le j \le 4$, with the identification $v_0 = v_4$ as shown in Fig. 1. Throughout the paper, all quadrilaterals are assumed to be convex. Set $P_1(Q) = \mathrm{Span}\{1,\, x_1,\, x_2\}$. Then the following holds [14]:

Proposition 3.1 *Let $Q \in \mathbb{R}^2$ be a quadrilateral. If $u \in P_1(Q)$, then $u(m_1) + u(m_3) = u(m_2) + u(m_4)$. Conversely, if u_j is a given value at m_j for $1 \le j \le 4$, satisfying $u_1+u_3 = u_2+u_4$, then there is a unique $u \in P_1(Q)$ such that $u(m_j) = u_j$, $1 \le j \le 4$.*

For $1 \le j \le 4$, let $\widehat{\phi}_j \in P_1(Q)$ be defined such that

$$\widehat{\phi}_j(m_k) = \begin{cases} 1, & k = j,\, j+1 \pmod 4, \\ 0, & \text{otherwise.} \end{cases} \tag{3.1}$$

For examples, if Q is the unit square $[-1,\, 1]^2$ with the midpoints $m_1(0,\, -1)$, $m_2(1,\, 0)$, $m_3(0,\, 1)$ and $m_4(-1,\, 0)$, then $\widehat{\phi}_1(x_1,\, x_2) = (1/2)(1+x_1-x_2)$. The following holds [14]:

Proposition 3.2 $\mathrm{Span}\{\widehat{\phi_1},\, \widehat{\phi_2},\, \widehat{\phi_3}, \widehat{\phi_4}\} = P_1(Q)$. *Indeed, any three of $\widehat{\phi_1},\, \widehat{\phi_2},\, \widehat{\phi_3},\, \widehat{\phi_4}$ span $P_1(Q)$.*

Notice that the centroid C in Fig. 1 is indeed the center of the four vertices of equal mass [9]. Given a two-dimensional decomposition $\mathcal{T}_h^2$ of

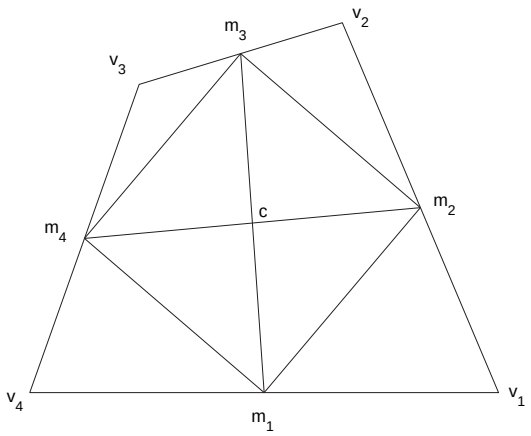

Fig. 1. The midpoints m_j, $1 \le j \le 4$, forms a parallelogram in the quadrilateral with vertices v_j, $1 \le j \le 4$, and C denotes their centroid.

$\Omega \subset \mathbb{R}^2$ into nonoverlapping quadrilaterals, let N_Q, N_V, and N_E denote the numbers of quadrilaterals, vertices, and edges, respectively, in $\mathcal{T}_h^2$. Then set

$$\mathcal{T}_h^2 = \{Q_1, Q_2, \ldots, Q_{N_Q}\}; \quad \bigcup_{j=1}^{N_Q} \overline{Q}_j = \overline{\Omega},$$
$$\mathcal{V}_h^2 = \{v_1, v_2, \ldots, v_{N_V}\}\text{: the set of all vertices of in } \mathcal{T}_h^2,$$
$$\mathcal{E}_h^2 = \{s_1, s_2, \ldots, s_{N_E}\}\text{: the set of all edges in } \mathcal{T}_h^2,$$
$$\mathcal{M}_h^2 = \{m_1, m_2, \ldots, m_{N_E}\}\text{: the set of all edge-midpoints in } \mathcal{T}_h^2.$$

For each vertex $v_j \in \mathcal{V}_h^2$, $\mathcal{E}_h^2(j)$ denotes the set of all edges $e \in \mathcal{E}_h^2$ which contain the vertex v_j, and $\mathcal{M}_h^2(j)$ the set of all midpoints m in $\mathcal{E}_h^2(j)$. Set

$$\mathcal{N}C_h^2 = \{v_h\colon v_h|_Q \in P_1(Q) \text{ for all } Q \in \mathcal{T}_h^2,\ v_h \text{ is continuous on } \mathcal{M}_h^2\}.$$

Let $\phi_j \in \mathcal{N}C_h^2$ be defined by

$$\phi_j(m) = \begin{cases} 1 & \text{if } m \in \mathcal{M}_h^2(j), \\ 0 & \text{if } m \in \mathcal{M}_h^2 \setminus \mathcal{M}_h^2(j). \end{cases} \tag{3.2}$$

The dimension and basis functions for $\mathcal{N}C_h^2$ for the two-dimensional case are given as follows [14].

Theorem 3.3 *Let ϕ_j be the function defined in* (3.2) *with each vertex $v_j \in \mathcal{V}_h^2$, $j = 1, \ldots, N_V$. Choose any vertex $v_{j_0} \in \mathcal{V}_h^2$. Then $\{\phi_1, \phi_2, \ldots, \phi_{N_V}\} \setminus \{\phi_{j_0}\}$ forms a basis for $\mathcal{NC}_h^2$. Moreover,* $\dim(\mathcal{NC}_h^2) = N_E - N_Q = N_V - 1$. *That is, the degrees of freedom for $\mathcal{NC}_h^2$ are equal to the number of vertices in $\mathcal{T}_h^2$ minus* 1.

Proof. The proof is given in [14] using a dimensional argument with dual basis. Instead, here we will give a short proof. Notice that the total degrees of freedom are equal to the number of edges in Ω_h minus the number of restrictions that the sum of values at the opposite midpoints should be equal in every quadrilateral, that is, $N_E - N_Q$. By Euler formula, it is equal to $N_V - 1$. It is an easy consequence of dimensional argument that $\{\phi_1, \phi_2, \ldots, \phi_{N_V}\} \setminus \{\phi_{j_0}\}$ forms a basis for $\mathcal{NC}_h^2$. □

3.2. The P_1-nonconforming element on hexahedron

We turn to three dimension. Consider an arbitrary hexahedron H, and, for $j = 1, \ldots, 6$, let c_j be the centroid of each face of H. By a centroid of face, we will mean the centroid of the four vertices of face. For example, if v_1, v_2, v_3, v_4 are the vertices of a face of H, then the centroid c of the face is defined by

$$c = \frac{v_1 + v_2 + v_3 + v_4}{4}. \tag{3.3}$$

Moreover, assume that c_j and c_k are opposite if $j + k = 7$ as shown in Fig. 2. Then one has the following [14]:

Proposition 3.4 *Let $H \in \mathbb{R}^3$ be a hexahedron with centroids c_j, $j = 1, \ldots, 6$. If $u \in P_1(H)$, then*

$$u(c_1) + u(c_6) = u(c_2) + u(c_5) = u(c_3) + u(c_4). \tag{3.4}$$

Conversely, if u_j is a given value at c_j for $1 \le j \le 6$, satisfying $u_1 + u_6 = u_2 + u_5 = u_3 + u_4$, then there is a unique $u \in P_1(H)$ such that $u(c_j) = u_j$, $1 \le j \le 6$.

For $1 \le j \le 8$, associated with the vertex v_j of H let $\widehat{\phi} \in P_1(H)$ be defined such that

$$\widehat{\phi}_j(c_k) = \begin{cases} 1 & \text{at the centroid of face whose vertices contain } v_j, \\ 0 & \text{at the centroid of face} \\ & \qquad \text{whose vertices does not contain } v_j. \end{cases}$$

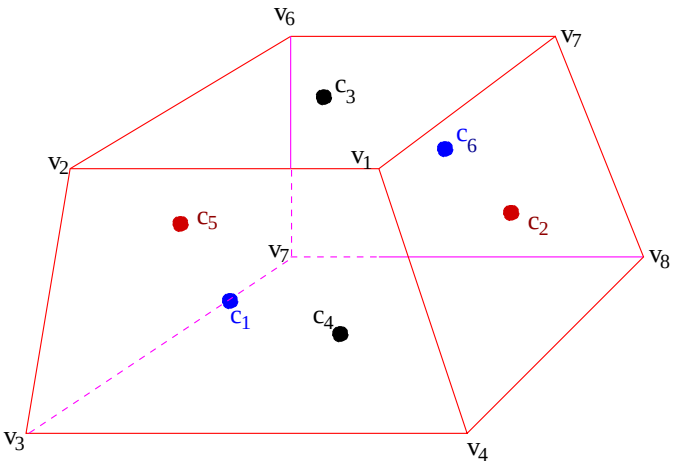

Fig. 2. v_j denote the vertices, $j = 1, \ldots, 8$, and c_k the centroids of the faces, $k = 1, \ldots, 6$.

Then the following holds [7]:

Proposition 3.5 $\mathrm{Span}\{\widehat{\phi_1}, \widehat{\phi_2}, \ldots, \widehat{\phi_8}\} = P_1(H)$. *Indeed there exist four among* $\widehat{\phi_1}, \widehat{\phi_2}, \ldots, \widehat{\phi_8}$ *which span* $P_1(H)$.

Given a three-dimensional decomposition $\mathcal{T}_h^3$ of $\Omega \subset \mathbb{R}^3$ into nonoverlapping hexahedrons, let N_H, N_F, N_V, and N_E denote the numbers of hexahedrons, faces, vertices, and edges, respectively, in $\mathcal{T}_h^3$. Then set

$$\mathcal{T}_h^3 = \{H_1, H_2, \ldots, H_{N_H}\}; \quad \bigcup_{j=1}^{N_H} \overline{H}_j = \overline{\Omega},$$

$$\mathcal{H}_h^3 = \{H_1, H_2, \ldots, H_{N_H}\}: \text{the set of all hexahedrons } H \in \mathcal{T}_h^3,$$

$$\mathcal{F}_h^3 = \{F_1, F_2, \ldots, F_{N_F}\}: \text{the set of all faces in } \mathcal{T}_h^3,$$

$$\mathcal{V}_h^3 = \{v_1, v_2, \ldots, v_{N_V}\}: \text{the set of all vertices in } \mathcal{T}_h^3,$$

$$\mathcal{M}_h^3 = \{m_1, m_2, \ldots, m_{N_F}\}: \text{the set of all centroids of faces } F_j \in \mathcal{F}_h^3.$$

For each vertex $v_j \in \mathcal{V}_h^3$, $\mathcal{F}_h^3(j)$ denotes the set of all faces $f \in \mathcal{F}_h^3$ whose vertices contain v_j, and $\mathcal{M}_h^3(j)$ the set of all centroids m in $\mathcal{F}_h^3(j)$. Set

$$\mathcal{NC}_h^3 = \{v_h : v_h|_Q \in P_1(Q) \text{ for all } Q \in \mathcal{T}_h^3, v_h \text{ is continuous on } \mathcal{M}_h^3\}.$$

Let $\phi_j \in \mathcal{NC}_h^3$ be defined by

$$\phi_j(m) = \begin{cases} 1 & \text{if } m \in \mathcal{M}_h^3(j), \\ 0 & \text{if } m \in \mathcal{M}_h^3 \setminus \mathcal{M}_h^3(j). \end{cases} \tag{3.5}$$

Similarly to the two-dimensional case, the dimension for $\mathcal{NC}_h^3$ is given as follows [7]:

Theorem 3.6 *Let N_F and N_H denote the numbers of faces and hexahedrons in $\mathcal{NC}_h^3$. Then*

$$\dim(\mathcal{NC}_h^3) = N_F - 2N_H. \tag{3.6}$$

That is, the degrees of freedom for $\mathcal{NC}_h^3$ are equal to the number of faces in $\mathcal{T}_h^3$ minus twice that of hexahedrons.

Proof. Notice that the total degrees of freedom are equal to the number of faces in Ω_h minus the number of restrictions that the sum of values at the opposite midpoints should be equal in every hexahedron, that is, $N_F - 2N_H$. □

4. Numerical dispersion of P_1-NC finite element solutions

From now on, we denote by $\mathcal{NC}_h^n$ the P_1 NC finite element space $\mathcal{NC}_h^2$ or $\mathcal{NC}_h^3$ depending on its dimension n. The nonconforming Galerkin approximation is then to find the solution $u_h \in \mathcal{NC}_h^n$ of the equation

$$a_h(u_h, v) = F(v), \quad \forall v \in \mathcal{NC}_h^n, \tag{4.1}$$

where

$$a_h(u, v) = -\Big(\frac{\omega^2}{c^2}u, v\Big) + \sum_{Q \in \mathcal{T}_h^n} (\nabla u, \nabla v)_Q + i\omega \Big\langle\Big\langle \frac{1}{c}u, v \Big\rangle\Big\rangle_\Gamma.$$

Here, and in what follows, $\Gamma = \cup_j \Gamma_j$ will mean the disjoint union of boundary edges in $\mathcal{T}_h^2$ or boundary faces in $\mathcal{T}_h^3$ of the domain Ω, and $\langle\langle u, v\rangle\rangle_\Gamma = \sum_j \langle\langle u, v\rangle\rangle_{\Gamma_j}$ with $\langle\langle \cdot, \cdot \rangle\rangle_{\Gamma_j}$ denoting the approximation to the complex inner product $\langle \cdot, \cdot \rangle_{\Gamma_j}$ in $L^2(\Gamma_j)$ by the one-point quadrature at the midpoint or centroid ξ_j of Γ_j:

$$\langle\langle u, v\rangle\rangle_{\Gamma_j} = (u\overline{v})(\xi_j)|\Gamma_j|.$$

For dispersion analysis, we follow the idea given in [20, 19], by setting the source term in (2.7) to zero and neglecting the boundary condition. Also

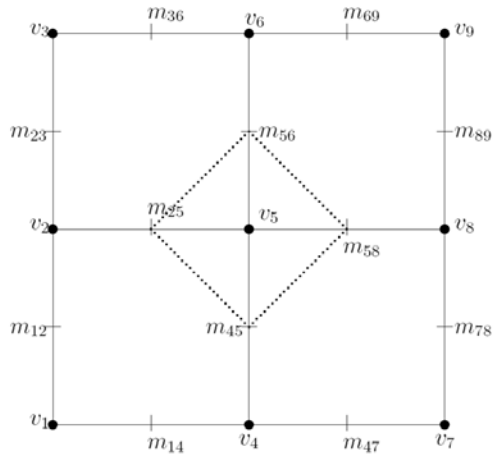

Fig. 3. v_j denotes the vertex and m_{jk} the midpoints of the vertices v_j and v_k. The global test function ϕ_G for P_1 NC element is constructed to have values 1 at m_{45}, m_{25}, m_{56}, m_{58} and 0 at the other midpoints.

c is assumed to be constant in the dispersion analysis. The weak formulation (4.1) is then reduced to

$$-\frac{\omega^2}{c^2}(u_h,\, v) + \sum_{Q\in\mathcal{T}_h^n} (\nabla u_h,\, \nabla v)_Q = 0, \quad \forall v \in \mathcal{NC}_h^n. \tag{4.2}$$

4.1. The two-dimensional case

Let us restrict ourselves to a portion of the domain far away from the artificial boundaries, say, $[-h,\, h]^2$, and then re-index the variables as shown in Fig. 3. Let $u_h(\mathbf{x},\, \omega) = \sum_{j=1}^{9} a_j \phi_j(\mathbf{x})$ and choose a test function $\phi = \phi_5$ in (4.2) to get

$$\begin{aligned} -\frac{\omega^2(h/2)^2}{c^2}\Big[&\frac{1}{3}a_1 + 2a_2 + \frac{1}{3}a_3 + 2a_4 \\ &+ \frac{20}{3}a_5 + 2a_6 + \frac{1}{3}a_7 + 2a_8 + \frac{1}{3}a_9\Big] \\ &+ \big[-2a_1 - 2a_3 + 8a_5 - 2a_7 - 2a_9\big] = 0. \end{aligned} \tag{4.3}$$

Here, as an example, we designate our global basis function ϕ_5 associated with the vertex v_5, as shown in Fig. 3, as the piecewise-linear polynomial:

$$\phi_5 = \begin{cases} \phi_{RB} & \text{in } \Omega_1, \\ \phi_{LB} & \text{in } \Omega_2, \\ \phi_{LT} & \text{in } \Omega_3, \\ \phi_{RT} & \text{in } \Omega_4, \end{cases} \tag{4.4}$$

where ϕ_{RB} is the linear polynomial in Ω_1 and have the value of which is 1 at m_{25}, m_{56} and 0 at m_{23}, m_{36}. The function values of ϕ_5 in the other elements are similarly defined. Consider the plane wave solution in the direction of propagation $\mathbf{k} = (k_1, k_2)$ of (2.7a) with $f = 0$ of the form

$$u(x_1, x_2, \omega) = e^{-i(k_1 x_1 + k_2 x_2)}, \tag{4.5}$$

with the dispersion relation $k_1^2 + k_2^2 = \omega^2/c^2$. To derive a numerical dispersion relation, we attempt to replace the coefficients a_i, $i = 1, \ldots, 9$, by the nodal values of the numerical solution $u_h(\mathbf{x}_{jk}, \omega) = e^{-i(\mathbf{k}^h \cdot \mathbf{x}_j)}$, $\mathbf{x}_j = v_j$, $j = 1, \ldots, 9$, with the numerical wave vector $\mathbf{k}^h = (k_1^h, k_2^h)$. Due to Proposition 3.1 and the definition (3.2) of basis functions, the coefficients a_k's should be determined by averaging the values of plane wave solutions at the two vertices which share an edge-midpoint.

For example, since the value at m_{12} of the numerical solution is determined by the values at v_1 and v_2, we also impose that the value at this midpoint be determined by the plane wave solutions at the vertices v_1 and v_2. Therefore, using

$$\begin{aligned} \frac{1}{2}\big[e^{i(k_1^h + k_2^h)h} + e^{ik_1^h h}\big] &= \frac{1}{2} e^{ik_1^h h}\big(1 + \cos(k_2^h h) + i \sin(k_2^h h)\big) \\ &= e^{i(k_1^h + k_2^h/2)h} \cos\Big(\frac{k_2^h h}{2}\Big), \end{aligned}$$

in order to reduce the numerical dispersion we have the requirement:

$$a_1 + a_2 = e^{i(k_1^h + k_2^h/2)h} \cos\Big(\frac{k_2^h h}{2}\Big). \tag{4.6}$$

The other midpoint values at $m'_{jk}s$ give similar relations, resulting, together with (4.6), in the following linear system for a_j, $j = 1, \ldots, 9$:

$$\begin{aligned} &a_1 + a_2 = e^{i(k_1^h + k_2^h/2)h} \cos\Big(\frac{k_2^h h}{2}\Big), \quad a_4 + a_5 = e^{i(k_2^h/2)h} \cos\Big(\frac{k_2^h h}{2}\Big), \\ &a_2 + a_5 = e^{i(k_1^h/2)h} \cos\Big(\frac{k_1^h h}{2}\Big), \quad a_1 + a_4 = e^{i(k_1^h/2 + k_2^h)h} \cos\Big(\frac{k_1^h h}{2}\Big), \end{aligned}$$

$$
\begin{aligned}
a_2 + a_3 &= e^{i(k_1^h - k_2^h/2)h} \cos\Big(\frac{k_2^h h}{2}\Big),\\
a_5 + a_6 &= e^{i(-k_2^h/2)h} \cos\Big(\frac{k_2^h h}{2}\Big),\\
a_3 + a_6 &= e^{i(k_1^h/2 - k_2^h)h} \cos\Big(\frac{k_1^h h}{2}\Big),\\
a_4 + a_7 &= e^{i(-k_1^h/2 + k_2^h)h} \cos\Big(\frac{k_1^h h}{2}\Big),\\
a_5 + a_8 &= e^{i(-k_1^h/2)h} \cos\Big(\frac{k_1^h h}{2}\Big),\\
a_6 + a_9 &= e^{i(-k_1^h/2 - k_2^h)h} \cos\Big(\frac{k_1^h h}{2}\Big),\\
a_7 + a_8 &= e^{i(-k_1^h + k_2^h/2)h} \cos\Big(\frac{k_2^h h}{2}\Big),\\
a_8 + a_9 &= e^{i(-k_1^h - k_2^h/2)h} \cos\Big(\frac{k_2^h h}{2}\Big).
\end{aligned}
\tag{4.7}
$$

One can verify that the above linear system (4.7) is consistent of rank 8: for instance, the first four equations in (4.7) are consistent and rank one deficient, and hence the fourth depends on the first three equations, and so on. Thus a_j, $j = 2, \ldots, 9$, can be written in terms of a_1 and h, k_1, k_2. A simple computation replacing the values of a_j, $j = 2, \ldots, 9$ in (4.3) leads to the numerical dispersion relation:

$$
\omega = \frac{2\sqrt{6}c}{h} \sqrt{\frac{1 - \cos(k_1^h h)\cos(k_2^h h)}{5 + 3(\cos(k_1^h h) + \cos(k_2^h h)) + \cos(k_1^h h)\cos(k_2^h h)}}. \tag{4.8}
$$

We summarize the above result as in the following theorem:

Theorem 4.1 *The dispersion relation for the P_1 nonconforming quadrilateral element method for the Helmholtz equation* (2.7a) *is given by* (4.8).

Remark 4.1 If the Q_1 conforming finite element is adopted, one has the following dispersion relation:

$$
\begin{aligned}
\omega &= \sqrt{12}\frac{c}{h}\\
&\times \sqrt{\frac{4 - \cos(k_1^h h) - \cos(k_2^h h) - \cos((k_1^h + k_2^h)h) - \cos((k_1^h - k_2^h)h)}{4(\cos(k_1^h h) + \cos(k_2^h h)) + \cos((k_1^h + k_2^h)h) + \cos((k_1^h - k_2^h)h) + 8}}.
\end{aligned}
\tag{4.9}
$$

Instead with the DSSY NC element employed, Zyserman, Gauzellino, and Santos obtained the following dispersion relation: [20]

$$\omega = 2\sqrt{6}\frac{c}{h}\sqrt{\frac{1-\cos(k_1^h h/2)\cos(k_2^h h/2)}{2+\cos(k_1^h h/2)\cos(k_2^h h/2)}}. \tag{4.10}$$

4.2. The three-dimensional case

In the three-dimensional case, we analyze the numerical dispersion relation with the numerical solution $u_h(x_1, x_2, x_3, \omega) = e^{-i(k_1^h x_1 + k_2^h x_2 + k_3^h x_3)}$, with the numerical wave number vector $\mathbf{k}^h = (k_1^h, k_2^h, k_3^h)$. Analogous to the two-dimensional case, the dispersion relation is derived as stated in the following theorem.

Theorem 4.2 *The dispersion relation for the P_1 nonconforming hexahedral element method for the Helmholtz equation* (2.7a) *is as follows*:

$$\omega = \sqrt{6}\frac{c}{h}\sqrt{\frac{3+A-B-3C}{3+2A+B}}, \tag{4.11}$$

where

$$\begin{aligned} A &= \cos(k_1^h h) + \cos(k_2^h h) + \cos(k_3^h h), \\ B &= \cos(k_1^h h)\cos(k_2^h h) + \cos(k_2^h h)\cos(k_3^h h) \\ &\qquad + \cos(k_3^h h)\cos(k_1^h h), \\ C &= \cos(k_1^h h)\cos(k_2^h h)\cos(k_3^h h). \end{aligned} \tag{4.12}$$

Proof. As in the two dimensional case, we restrict the computational domain to $[-h, h]^3$, which is then divided into eight congruent subcubes.

Introduce the following notations, a_{jkl}, $j, k, l = 0, \pm 1$, η_{jkl}, $j, k, l = 0, \pm 1, \pm 1/2$, R_{jkl}, $j, k, l = \pm$. To avoid possible confusion between arithmetics and indices, we will use the convention that j' means $-j$. For examples, $a_{101'}$ means the value at the vertex $(h, 0, -h)$, $\eta_{11/2'1/2}$ means the value at the point $(h, -h/2, h/2)$, and R_{+-+} represents the subcube $\{(x_1, x_2, x_3)\colon 0 < x_1 < h, -h < x_2 < 0, 0 < x_3 < 0\}$, and so on. Let $u_h(x_1, x_2, x_3, \omega) = \sum_{j,k,l=0,\pm 1} a_{jkl}\phi_j(x_1, x_2, x_3)$ and assume that $u_h(\mathbf{x}_j, \omega) = e^{-i\mathbf{k}^h\cdot\mathbf{x}_j}$ for all 27 vertices of the eight subcubes, where a_j's are determined by the function values at the centroid of 36 faces. We choose a test function $\phi = \phi_{000}$ in (4.2) to get

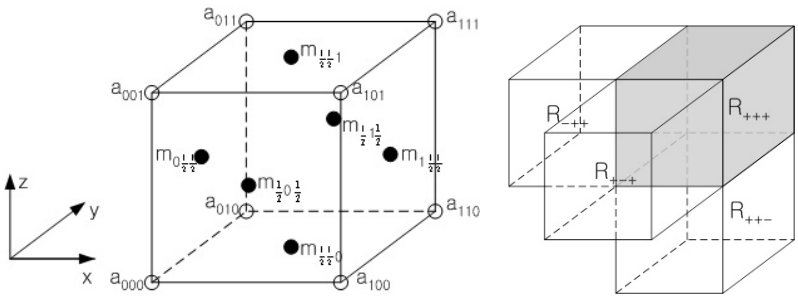

(a) (b)

Fig. 4. (a) a_{ijk} denotes the value at the vertex (ih, jk, kh), $i, j, k = 0, -1, 1$. η_{ijk} is the value at the centroid of the rectangular containing (ih, jk, kh), which i, j, k are one of 0, 1, $1'$, 1/2 and $(1/2)'$. Here $(1/2)'$ means $-1/2$. (b) the hexahedral element divided with the eight regions, which are R_{+++}, R_{++-}, R_{+-+}, R_{+--}, R_{-++}, R_{-+-}, R_{--+} and R_{---}.

$$
\begin{aligned}
-\frac{\omega^2(h/2)^3}{c^2}\Big[&\frac{8}{3}a_{01'1'} + \frac{8}{3}a_{1'01'} + \frac{32}{3}a_{001'} + \frac{8}{3}a_{101'} + \frac{8}{3}a_{011'} \\
&+ \frac{8}{3}a_{1'1'0} + \frac{32}{3}a_{01'0} + \frac{8}{3}a_{11'0} + \frac{32}{3}a_{1'00} + 32a_{000} \\
&+ \frac{32}{3}a_{100} + \frac{8}{3}a_{1'10} + \frac{32}{3}a_{010} + \frac{8}{3}a_{110} + \frac{8}{3}a_{01'1} \\
&+ \frac{8}{3}a_{1'01} + \frac{32}{3}a_{001} + \frac{8}{3}a_{101} + \frac{8}{3}a_{011}\Big] \\
+\frac{h}{2}[&-6a_{1'1'1'} - 4a_{01'1'} - 6a_{11'1'} - 4a_{1'01'} + 8a_{001'} - 4a_{101'} \\
&- 6a_{1'11'} - 4a_{011'} - 6a_{111'} + 8a_{01'0} + 8a_{1'00} + 48a_{000} \\
&+ 8a_{100} + 8a_{010} - 6a_{1'1'1} - 4a_{01'1} - 6a_{11'1} - 4a_{1'01} \\
&+ 8a_{001} - 4a_{101} - 6a_{1'11} - 4a_{011} - 6a_{111}] = 0. \qquad (4.13)
\end{aligned}
$$

Consider the approximation at the centroid $(h, h/2, h/2)$. The value at this centroid is determined by the values of plane wave solution at the four vertices of the face containing the centroid. In the region $R_{+++} := \{(x_1, x_2, x_3) : 0 \le x_1, x_2, x_3 \le h\}$, the 6 centroids determine 6 equations. Utilizing the following type of trigonometry,

$$\begin{aligned}
&\frac{1}{4}\big[e^{-ik_1^h h} + e^{-i(k_1^h+k_2^h)h} + e^{-i(k_1^h+k_3^h)h} + e^{-i(k_1^h+k_2^h+k_3^h)h}\big] \qquad (4.14)\\
&= e^{-ik_1^h h}\frac{1 + e^{-ik_2^h h} + e^{-ik_3^h h} + e^{-i(k_2^h+k_3^h)h}}{4}\\
&= e^{-i(k_1^h+k_2^h/2+k_3^h/2)h}\cos\Big(\frac{k_2^h h}{2}\Big)\cos\Big(\frac{k_3^h h}{2}\Big),
\end{aligned}$$

one can write

$$\begin{aligned}
&a_{100} + a_{110} + a_{101} + a_{111}\\
&\quad = e^{-i(k_1^h+k_2^h/2+k_3^h/2)h}\cos\Big(\frac{k_2^h h}{2}\Big)\cos\Big(\frac{k_3^h h}{2}\Big) := \eta_{1\frac12\frac12}, \qquad (4.15a)\\
&a_{010} + a_{110} + a_{011} + a_{111}\\
&\quad = e^{-i(k_1^h/2+k_2^h+k_3^h/2)h}\cos\Big(\frac{k_1^h h}{2}\Big)\cos\Big(\frac{k_3^h h}{2}\Big) := \eta_{\frac121\frac12}, \qquad (4.15b)\\
&a_{001} + a_{101} + a_{011} + a_{111}\\
&\quad = e^{-i(k_1^h/2+k_2^h/2+k_3^h)h}\cos\Big(\frac{k_1^h h}{2}\Big)\cos\Big(\frac{k_2^h h}{2}\Big) := \eta_{\frac12\frac121}, \qquad (4.15c)\\
&a_{000} + a_{100} + a_{010} + a_{110}\\
&\quad = e^{-i(k_1^h/2+k_2^h/2)h}\cos\Big(\frac{k_1^h h}{2}\Big)\cos\Big(\frac{k_2^h h}{2}\Big) := \eta_{\frac12\frac120}, \qquad (4.15d)\\
&a_{000} + a_{010} + a_{001} + a_{011}\\
&\quad = e^{-i(k_2^h/2+k_3^h/2)h}\cos\Big(\frac{k_2^h h}{2}\Big)\cos\Big(\frac{k_3^h h}{2}\Big) := \eta_{0,\frac12,\frac12}, \qquad (4.15e)\\
&a_{000} + a_{100} + a_{001} + a_{101}\\
&\quad = e^{-i(k_1^h/2+k_3^h/2)h}\cos\Big(\frac{k_1^h h}{2}\Big)\cos\Big(\frac{k_3^h h}{2}\Big) := \eta_{\frac120\frac12}. \qquad (4.15f)
\end{aligned}$$

Notice that the six equations in (4.15) are of rank 4, but consistent. Using only the four linearly independent equations (4.15f), (4.15e), (4.15d) and (4.15c), the following four values at the vertices can be expressed in terms of the other four vertex values and the values at the centroids:

$$\begin{aligned}
a_{101} &= \eta_{\frac120\frac12} - (a_{000} + a_{100} + a_{001}), \qquad (4.16a)\\
a_{011} &= \eta_{0\frac12\frac12} - (a_{000} + a_{010} + a_{001}), \qquad (4.16b)\\
a_{110} &= \eta_{\frac12\frac120} - (a_{000} + a_{100} + a_{010}), \qquad (4.16c)\\
a_{111} &= \eta_{\frac12\frac121} - (a_{001} + a_{101} + a_{011})\\
&= \eta_{\frac12\frac121} - (a_{001} + \eta_{\frac120\frac12} - (a_{000} + a_{100} + a_{001})\\
&\qquad + \eta_{0\frac12\frac12} - (a_{000} + a_{010} + a_{001}))
\end{aligned}$$

$$= \eta_{\frac{1}{2}\frac{1}{2}1} - \eta_{\frac{1}{2}0\frac{1}{2}} - \eta_{0\frac{1}{2}\frac{1}{2}} + (2a_{000} + a_{100} + a_{010} + a_{001}). \quad (4.16d)$$

Now, we consider the other three subcubes each of which shares a centroid of R_{+++}, say, R_{-++}, R_{+-+}, R_{++-} (Fig. 4). Each subcube has additional 5 centroids. Similarly to the above, the following equations are obtained on the region R_{-++}:

$$\begin{aligned}
&a_{1'00} + a_{1'10} + a_{1'01} + a_{1'11} \\
&\quad = e^{-i(-k_1^h + k_2^h/2 + k_3^h/2)h} \cos\Big(\frac{k_2^h h}{2}\Big) \cos\Big(\frac{k_3^h h}{2}\Big) := \eta_{1'\frac{1}{2}\frac{1}{2}}, && (4.17a)\\
&a_{010} + a_{1'10} + a_{0,1,1} + a_{1'11} \\
&\quad = e^{-i(-k_1^h/2 + k_2^h + k_3^h/2)h} \cos\Big(\frac{k_1^h h}{2}\Big) \cos\Big(\frac{k_3^h h}{2}\Big) := \eta_{\frac{1}{2}'1\frac{1}{2}}, && (4.17b)\\
&a_{001} + a_{1'01} + a_{011} + a_{1'11} \\
&\quad = e^{-i(-k_1^h/2 + k_2^h 2 + k_3^h)h} \cos\Big(\frac{k_1^h h}{2}\Big) \cos\Big(\frac{k_2^h h}{2}\Big) := \eta_{\frac{1}{2}'\frac{1}{2}1}, && (4.17c)\\
&a_{000} + a_{1'00} + a_{010} + a_{1'10} \\
&\quad = e^{-i(-k_1^h/2 + k_2^h/2)h} \cos\Big(\frac{k_1^h h}{2}\Big) \cos\Big(\frac{k_2^h h}{2}\Big) := \eta_{\frac{1}{2}'\frac{1}{2}0}, && (4.17d)\\
&a_{000} + a_{1'00} + a_{001} + a_{1'01} \\
&\quad = e^{-i(-k_1^h/2 + k_3^h/2)h} \cos\Big(\frac{k_1^h h}{2}\Big) \cos\Big(\frac{k_3^h h}{2}\Big) := \eta_{\frac{1}{2}'0\frac{1}{2}}. && (4.17e)
\end{aligned}$$

The argument from (4.15) to (4.16) will apply to (4.17), and in this case, we have additional three (instead of four) independent relations which provide the following relations:

$$\begin{aligned}
a_{1'01} &= \eta_{\frac{1}{2}'0\frac{1}{2}} - (a_{000} + a_{1'00} + a_{001}), && (4.18a)\\
a_{1'10} &= \eta_{\frac{1}{2}'\frac{1}{2}0} - (a_{000} + a_{1'00} + a_{010}), && (4.18b)\\
a_{1'11} &= \eta_{\frac{1}{2}'\frac{1}{2}1} - (a_{001} + a_{1'01} + a_{011}) \\
&= \eta_{\frac{1}{2}'\frac{1}{2}1} - \big(a_{001} + \eta_{\frac{1}{2}'0\frac{1}{2}} - (a_{000} + a_{1'00} + a_{001}) \\
&\qquad + \eta_{0\frac{1}{2}\frac{1}{2}} - (a_{000} + a_{010} + a_{001})\big) \\
&= \eta_{\frac{1}{2}'\frac{1}{2}1} - \eta_{\frac{1}{2}'0\frac{1}{2}} - \eta_{0\frac{1}{2}\frac{1}{2}} + (2a_{000} + a_{1'00} + a_{010} + a_{001}). && (4.18c)
\end{aligned}$$

notice that there are some patterns. Similarly, on each R_{+-+} and R_{++-}, five equations of type (4.17) and three equations of type (4.18) can be derived.

Next, we consider the regions R_{--+}, R_{+--} and R_{-+-}. Each region has four equations which reduce to two relations between vertex-wise values

and values at centroids:

$$
\begin{aligned}
&a_{1'00}+a_{1'1'0}+a_{1'01}+a_{1'1'1}\\
&\qquad = e^{-i(-k_1^h-k_2^h/2+k_3^h/2)h}\cos\Big(\frac{k_2^h h}{2}\Big)\cos\Big(\frac{k_3^h h}{2}\Big) := \eta_{1'\frac12'\frac12},\\
&a_{01'0}+a_{1'1'0}+a_{01'1}+a_{1'1'1}\\
&\qquad = e^{-i(-k_1^h/2-k_2^h+k_3^h/2)h}\cos\Big(\frac{k_1^h h}{2}\Big)\cos\Big(\frac{k_3^h h}{2}\Big) := \eta_{\frac12'1'\frac12},\\
&a_{001}+a_{1'01}+a_{01'1}+a_{1'1'1}\\
&\qquad = e^{-i(-k_1^h/2-k_2^h/2+k_3^h)h}\cos\Big(\frac{k_1^h h}{2}\Big)\cos\Big(\frac{k_2^h h}{2}\Big) := \eta_{\frac12'\frac12'1},\\
&a_{000}+a_{1'00}+a_{01'0}+a_{1'1'0}\\
&\qquad = e^{-i(-k_1^h/2-k_2^h/2)h}\cos\Big(\frac{k_1^h h}{2}\Big)\cos\Big(\frac{k_2^h h}{2}\Big) := \eta_{\frac12'\frac12'0}.
\end{aligned}
$$

and

$$
\begin{aligned}
a_{1'1'0} &= \eta_{\frac12'\frac12'0}-(a_{000}+a_{1'00}+a_{01'0}),\\
a_{1'1'1} &= \eta_{\frac12'\frac12'1}-(a_{001}+a_{1'01}+a_{01'1}),\\
&= \eta_{\frac12'\frac12'1}-\big(a_{001}+\eta_{\frac12'0\frac12}-(a_{000}+a_{1'00}+a_{001})\\
&\qquad\qquad +\eta_{0\frac12'\frac12}-(a_{000}+a_{01'0}+a_{001})\big)\\
&= \eta_{\frac12'\frac12'1}-\eta_{\frac12'0\frac12}-\eta_{0\frac12'\frac12}+(2a_{000}+a_{1'00}+a_{01'0}+a_{001}).
\end{aligned}
$$

Finally, we consider the region R_{---}. Similarly, the following three equations and one relation can be obtained:

$$
\begin{aligned}
&a_{1'00}+a_{1'1'0}+a_{1'01'}+a_{1'1'1'}\\
&\qquad = e^{-i(-k_1^h-k_2^h/2-k_3^h/2)h}\cos\Big(\frac{k_2^h h}{2}\Big)\cos\Big(\frac{k_3^h h}{2}\Big) := \eta_{1'\frac12'\frac12'},\\
&a_{01'0}+a_{1'1'0}+a_{01'1'}+a_{1'1'1'}\\
&\qquad = e^{-i(-k_1^h/2-k_2^h-k_3^h/2)h}\cos\Big(\frac{k_1^h h}{2}\Big)\cos\Big(\frac{k_3^h h}{2}\Big) := \eta_{\frac12'1'\frac12'},\\
&a_{001'}+a_{1'01'}+a_{01'1'}+a_{1'1'1'}\\
&\qquad = e^{-i(-k_1^h/2-k_2^h/2-k_3^h)h}\cos\Big(\frac{k_1^h h}{2}\Big)\cos\Big(\frac{k_2^h h}{2}\Big) := \eta_{\frac12'\frac12'1'},
\end{aligned}
$$

and

$$
a_{1'1'1'} = \eta_{\frac12'\frac12'1'}-(a_{001'}+a_{1'01'}+a_{01'1'})
$$

$$
\begin{aligned}
&= \eta_{\frac{1}{2}'\frac{1}{2}'1'} - \big(a_{001'} + \eta_{\frac{1}{2}'0\frac{1}{2}'} - (a_{000} + a_{1'00} + a_{001'}) \\
&\qquad + \eta_{0\frac{1}{2}'\frac{1}{2}'} - (a_{000} + a_{01'0} + a_{001'})\big) \\
&= \eta_{\frac{1}{2}'\frac{1}{2}'1} - \eta_{\frac{1}{2}'0\frac{1}{2}'} - \eta_{0\frac{1}{2}'\frac{1}{2}'} + (2a_{000} + a_{1'00} + a_{01'0} + a_{001'}).
\end{aligned}
$$

Up to now, we have total 36 equations and 20 relations. Notice that the degrees of freedom are indeed 20 as stated in Theorem 3.6. Set

$$
\begin{aligned}
G_1 &= a_{100} + a_{010} + a_{001} + a_{1'00} + a_{01'0} + a_{001'}, \\
G_2 &= a_{110} + a_{011} + a_{101} + a_{1'10} + a_{1'01} + a_{11'0} \\
&\quad + a_{01'1} + a_{101'} + a_{011'} + a_{1'1'0} + a_{01'1'} + a_{1'01'}, \\
G_3 &= a_{111} + a_{1'11} + a_{11'1} + a_{111'} + a_{1'1'1} + a_{11'1'} + a_{1'11'} + a_{1'1'1'}.
\end{aligned}
$$

Then by using the 20 relations, one can rewrite G_2 and G_3 as follows:

$$
\begin{aligned}
G_2 &= \eta_{0\frac{1}{2}\frac{1}{2}} + \eta_{0\frac{1}{2}\frac{1}{2}'} + \eta_{0\frac{1}{2}'\frac{1}{2}} + \eta_{0\frac{1}{2}'\frac{1}{2}'} + \eta_{\frac{1}{2}0\frac{1}{2}} + \eta_{\frac{1}{2}0\frac{1}{2}'} + \eta_{\frac{1}{2}'0\frac{1}{2}} \\
&\quad + \eta_{\frac{1}{2}'0\frac{1}{2}'} + \eta_{\frac{1}{2}\frac{1}{2}0} + \eta_{\frac{1}{2}\frac{1}{2}'0} + \eta_{\frac{1}{2}'\frac{1}{2}0} + \eta_{\frac{1}{2}'\frac{1}{2}'0} - 12a_{000} - 4G_1, \\
G_3 &= \eta_{\frac{1}{2}\frac{1}{2}1} + \eta_{\frac{1}{2}\frac{1}{2}1'} + \eta_{\frac{1}{2}\frac{1}{2}'1} + \eta_{\frac{1}{2}'\frac{1}{2}1} + \eta_{\frac{1}{2}\frac{1}{2}'1'} + \eta_{\frac{1}{2}'\frac{1}{2}1'} + \eta_{\frac{1}{2}'\frac{1}{2}'1} \\
&\quad + \eta_{\frac{1}{2}'\frac{1}{2}'1'} - 2(\eta_{0\frac{1}{2}\frac{1}{2}} + \eta_{0\frac{1}{2}\frac{1}{2}'} + \eta_{0\frac{1}{2}'\frac{1}{2}} + \eta_{0\frac{1}{2}'\frac{1}{2}'} + \eta_{\frac{1}{2}0\frac{1}{2}} + \eta_{\frac{1}{2}'0\frac{1}{2}} \\
&\quad + \eta_{\frac{1}{2}0\frac{1}{2}'} + \eta_{\frac{1}{2}'0\frac{1}{2}'}) + 16a_{000} + 4G_1.
\end{aligned}
$$

Similarly to the process of reducing the equation (4.3) in the two-dimensional case, one can deduce from (4.13) that

$$
\omega = \sqrt{3}\frac{c}{h}\sqrt{\frac{24a_{000} + 4G_1 - 2G_2 - 3G_3}{12a_{000} + 4G_1 + G_2}}. \tag{4.19}
$$

Observe that in the expression (4.19) the numerator and denominator in the square root are independent of a_{000} and G_1, but dependent only on η's: more precisely,

$$
\begin{aligned}
&24a_{000} + 4G_1 - 2G_2 - 3G_3 \qquad (4.20a) \\
&= 4\big(\eta_{0\frac{1}{2}\frac{1}{2}} + \eta_{0\frac{1}{2}\frac{1}{2}'} + \eta_{0\frac{1}{2}'\frac{1}{2}} + \eta_{0\frac{1}{2}'\frac{1}{2}'} + \eta_{\frac{1}{2}0\frac{1}{2}} + \eta_{\frac{1}{2}'0\frac{1}{2}} \\
&\qquad + \eta_{\frac{1}{2}0\frac{1}{2}'} + \eta_{\frac{1}{2}'0\frac{1}{2}'}\big) - 3\big(\eta_{\frac{1}{2}\frac{1}{2}1} + \eta_{\frac{1}{2}\frac{1}{2}1'} + \eta_{\frac{1}{2}'\frac{1}{2}'1} + \eta_{\frac{1}{2}'\frac{1}{2}'1'} \\
&\quad + \eta_{\frac{1}{2}'\frac{1}{2}1} + \eta_{\frac{1}{2}'\frac{1}{2}1'} + \eta_{\frac{1}{2}\frac{1}{2}'1} + \eta_{\frac{1}{2}\frac{1}{2}'1'}\big) \\
&\quad - 2\big(\eta_{\frac{1}{2}\frac{1}{2}0} + \eta_{\frac{1}{2}'\frac{1}{2}0} + \eta_{\frac{1}{2}\frac{1}{2}'0} + \eta_{\frac{1}{2}'\frac{1}{2}'0}\big), \\
&12a_{000} + 4G_1 + G_2 \qquad (4.20b)
\end{aligned}
$$

$$
\begin{aligned}
&= \eta_{0\frac12\frac12} + \eta_{0\frac12\frac12'} + \eta_{0\frac12'\frac12} + \eta_{0\frac12'\frac12'} + \eta_{\frac120\frac12} + \eta_{\frac12'0\frac12} \\
&\quad + \eta_{\frac120\frac12'} + \eta_{\frac12'0\frac12'} + \eta_{\frac12\frac120} + \eta_{\frac12'\frac120} + \eta_{\frac12\frac12'0} + \eta_{\frac12'\frac12'0}.
\end{aligned}
$$

Using the elementary formulae from trigonometry

$$
\cos^2\Big(\frac{\theta}{2}\Big) = \frac{1+\cos(2\theta)}{2}, \quad \exp(-i\theta) + \exp(i\theta) = 2\cos(\theta),
$$

one sees that

$$
\begin{aligned}
\eta_{0\frac12\frac12} + \eta_{0\frac12\frac12'} &= 2\cos\Big(\frac{k_2^h h}{2}\Big)\cos^2\Big(\frac{k_3^h h}{2}\Big)e^{-i(k_2^h/2)h}, \\
\eta_{0\frac12'\frac12} + \eta_{0\frac12'\frac12'} &= 2\cos\Big(\frac{k_2^h h}{2}\Big)\cos^2\Big(\frac{k_3^h h}{2}\Big)e^{i(k_2^h/2)h}, \\
\eta_{\frac120\frac12} + \eta_{\frac12'0\frac12} &= 2\cos^2\Big(\frac{k_1^h h}{2}\Big)\cos\Big(\frac{k_3^h h}{2}\Big)e^{-i(k_3^h/2)h}, \\
\eta_{\frac120\frac12'} + \eta_{\frac12'0\frac12'} &= 2\cos^2\Big(\frac{k_1^h h}{2}\Big)\cos\Big(\frac{k_3^h h}{2}\Big)e^{i(k_3^h/2h)},
\end{aligned}
$$

and therefore,

$$
\begin{aligned}
&\eta_{0\frac12\frac12} + \eta_{0\frac12\frac12'} + \eta_{0\frac12'\frac12} + \eta_{0\frac12'\frac12'} + \eta_{\frac120\frac12} + \eta_{\frac12'0\frac12} + \eta_{\frac120\frac12'} + \eta_{\frac12'0\frac12'} \\
&= 4\cos^2\Big(\frac{k_2^h h}{2}\Big)\cos^2\Big(\frac{k_3^h h}{2}\Big) + 4\cos^2\Big(\frac{k_1^h h}{2}\Big)\cos^2\Big(\frac{k_3^h h}{2}\Big) \\
&= (1+\cos(k_2^h h))(1+\cos(k_3^h h)) \\
&\quad + (1+\cos(k_1^h h))(1+\cos(k_3^h h)).
\end{aligned} \tag{4.21}
$$

Similarly,

$$
\begin{aligned}
\eta_{\frac12\frac121} + \eta_{\frac12\frac12 1'} &= 2\cos\Big(\frac{k_1^h h}{2}\Big)\cos\Big(\frac{k_2^h h}{2}\Big)e^{-i(k_1^h/2+k_2^h/2)h}\cos(k_3^h h), \\
\eta_{\frac12'\frac121} + \eta_{\frac12'\frac12 1'} &= 2\cos\Big(\frac{k_1^h h}{2}\Big)\cos\Big(\frac{k_2^h h}{2}\Big)e^{-i(-k_1^h/2+k_2^h/2)h}\cos(k_3^h h), \\
\eta_{\frac12'\frac12'1} + \eta_{\frac12'\frac12'1'} &= 2\cos\Big(\frac{k_1^h h}{2}\Big)\cos\Big(\frac{k_2^h h}{2}\Big)e^{-i(-k_1^h/2-k_2^h/2)h}\cos(k_3^h h), \\
\eta_{\frac12\frac12'1} + \eta_{\frac12\frac12'1'} &= 2\cos\Big(\frac{k_1^h h}{2}\Big)\cos\Big(\frac{k_2^h h}{2}\Big)e^{-i(k_1^h/2-k_2^h/2)h}\cos(k_3^h h),
\end{aligned}
$$

and hence

$$
\eta_{\frac12\frac121} + \eta_{\frac12\frac12 1'} + \eta_{\frac12'\frac121} + \eta_{\frac12'\frac12 1'}
$$

$$= 4\cos^2\Big(\frac{k_1^h h}{2}\Big)\cos\Big(\frac{k_2^h h}{2}\Big)e^{-i(k_2^h/2)h}\cos(k_3^h h),$$

$$\eta_{\frac12\,\frac12{}'1} + \eta_{\frac12{}'\frac12{}'1'} + \eta_{\frac12\,\frac12{}'1} + \eta_{\frac12{}'\frac12\,1'},$$

$$= 4\cos^2\Big(\frac{k_1^h h}{2}\Big)\cos\Big(\frac{k_2^h h}{2}\Big)e^{i(k_2^h/2)h}\cos(k_3^h h),$$

which implies that

$$\begin{aligned}
&\eta_{\frac12\,\frac12 1} + \eta_{\frac12\,\frac12 1'} + \eta_{\frac12{}'\frac12{}'1} + \eta_{\frac12{}'\frac12{}'1'} + \eta_{\frac12{}'\frac12 1} + \eta_{\frac12{}'\frac12 1'} + \eta_{\frac12\,\frac12{}'1} + \eta_{\frac12\,\frac12{}'1'}\\
&= 8\cos^2\Big(\frac{k_1^h h}{2}\Big)\cos^2\Big(\frac{k_2^h h}{2}\Big)\cos(k_3^h h)\\
&= 2(1+\cos(k_1^h h))(1+\cos(k_2^h h)\cos(k_3^h h). \qquad (4.22)
\end{aligned}$$

Also, since

$$\begin{aligned}
\eta_{\frac12\,\frac12 0} + \eta_{\frac12{}'\frac12 0} &= 2\cos^2\Big(\frac{k_1^h h}{2}\Big)\cos\Big(\frac{k_2^h h}{2}\Big)e^{-i(k_2^h/2)h},\\
\eta_{\frac12\,\frac12{}'0} + \eta_{\frac12{}'\frac12{}'0} &= 2\cos^2\Big(\frac{k_1^h h}{2}\Big)\cos\Big(\frac{k_2^h h}{2}\Big)e^{i(k_2^h/2)h},
\end{aligned}$$

one has

$$\begin{aligned}
&\eta_{\frac12\,\frac12 0} + \eta_{\frac12{}'\frac12 0} + \eta_{\frac12\,\frac12{}'0} + \eta_{\frac12{}'\frac12{}'0}\\
&\qquad = 4\cos^2\Big(\frac{k_1^h h}{2}\Big)\cos^2\Big(\frac{k_2^h h}{2}\Big)\\
&\qquad = (1+\cos(k_1^h h))(1+\cos(k_2^h h)). \qquad (4.23)
\end{aligned}$$

Thus, combining (4.20a) with (4.21)-(4.23). one arrives at

$$\begin{aligned}
&24a_{000} + 4G_1 - 2G_2 - 3G_3\\
&= 4\big((1+\cos(k_2^h h))(1+\cos(k_3^h h)) + (1+\cos(k_1^h h))(1+\cos(k_3^h h))\big)\\
&\quad - 6(1+\cos(k_1^h h))\\
&\quad \times (1+\cos(k_2^h h)\cos(k_3^h h) - 2(1+\cos(k_1^h h))(1+\cos(k_2^h h)))\\
&= 6 + 2A - 2B - 6C. \qquad (4.24)
\end{aligned}$$

Also, a combination of (4.20b) with (4.21) and (4.23) leads to

$$\begin{aligned}
&12a_{000} + 4G_1 + G_2 = (1+\cos(k_2^h h))(1+\cos(k_3^h h))\\
&\quad + (1+\cos(k_1^h h))(1+\cos(k_3^h h)) + (1+\cos(k_1^h h))(1+\cos(k_2^h h))\\
&= 3 + 2A + B. \qquad (4.25)
\end{aligned}$$

Finally, the equation (4.11) is a consequence of the equation (4.19) by applying the equations (4.24) and (4.25). □

Remark 4.2 If the three-dimensional Q_1 conforming finite element is adopted, one has the following dispersion relation:

$$\omega = \sqrt{18}\frac{c}{h}\sqrt{\frac{4-B-C}{8+4A+2B+C}}, \tag{4.26}$$

where the coefficients A, B, C are given by (4.12). If the three-dimensional DSSY NC element is used, Zyserman and Gauzellino show the following dispersion relation: [19]

$$\omega = 2\sqrt{3}\frac{c}{h}\sqrt{\frac{\beta_1^2\gamma_2\gamma_3+\beta_2^2\gamma_1\gamma_3+\beta_3^2\gamma_1\gamma_2}{(\gamma_1\gamma_2+\gamma_2\gamma_3+\gamma_3\gamma_1)}}, \tag{4.27}$$

where

$$\gamma_1 = \cos\Big(\frac{k_1^h h}{2}\Big), \quad \gamma_2 = \cos\Big(\frac{k_2^h h}{2}\Big), \quad \gamma_3 = \cos\Big(\frac{k_3^h h}{2}\Big),$$
$$\beta_1 = \sin\Big(\frac{k_1^h h}{2}\Big), \quad \beta_2 = \sin\Big(\frac{k_2^h h}{2}\Big), \quad \beta_3 = \sin\Big(\frac{k_3^h h}{2}\Big).$$

5. Analysis of the numerical dispersion

Let λ be the wavelength and G the number of grid points per wavelength such that $G = \lambda/h$. The dimensionless phase and group velocities, q and Q, are given by

$$q = \frac{1}{c}\frac{\omega}{|\mathbf{k}^h|}, \quad Q = \frac{1}{c}\nabla\omega \cdot \frac{1}{|\mathbf{k}^h|}\mathbf{k}^h. \tag{5.1}$$

Using the dispersion relations in Section 4, the phase and group velocities can be calculated depending on the elements adopted.

5.1. Dispersion curves according to the quadrilateral and hexahedral finite elements

In the two-dimensional case, we set $\mathbf{k}^h = (k_1^h, k_2^h) = k^h(\cos\theta, \sin\theta)$, here $k^h = |\mathbf{k}^h|$ is the numerical wave number $2\pi/\lambda$ and θ represents the direction of plane wave propagation, measured from the axis x_2. Fig. 5 shows the relation between the phase velocity q and the reciprocal of G with the propagation directions $\theta = 0, \pi/8, \pi/4$. From Fig. 5, we observe that among the three simplest finite elements the DSSY NC element requires

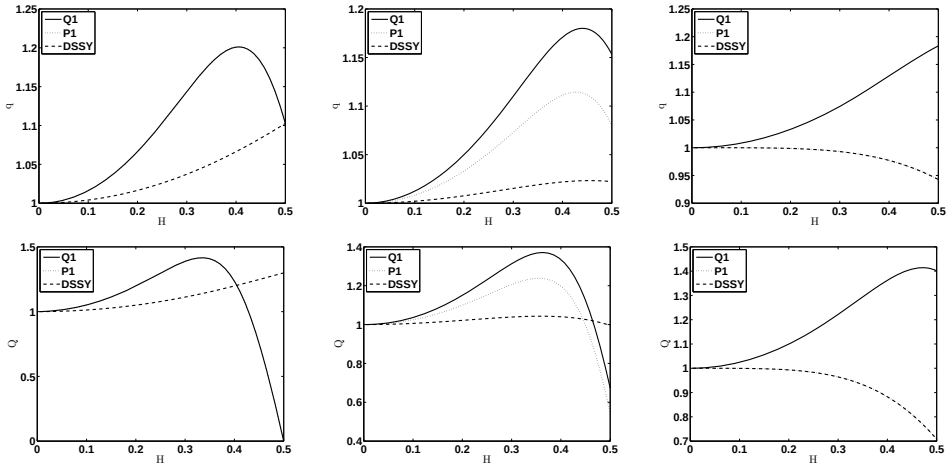

(a) $\theta = 0$ (b) $\theta = \pi/8$ (c) $\theta = \pi/4$

Fig. 5. Phase and group velocities for the two-dimensional problem. H in x-axis means the reciprocal of the number of grid points, and the values on y-axis are the phase and group velocities according to the propagation direction $\theta = 0, \pi/8, \pi/4$.

wave direction(θ)	Q_1 element	P_1 NC element	DSSY NC element
0	22.2	22.2	11.1
$\pi/8$	19.3	15.7	7.6
$\pi/4$	15.7	4.5	4.5

Table 1. The grid points G per wavelength needed the error within 1% in the two dimensional case.

the least number of grid points per wavelength to achieve certain accuracy. The behavior of dispersion relation of P_1 NC element is identical to that of Q_1 element for $\theta = 0$ (see Fig. 5(a)), and that of DSSY NC element for $\theta = \pi/4$ (see Fig. 5(c)). We also compute the number of grid points per wavelength needed in order to keep the error in group velocity within 1%. Taking into account of the grid points G per wavelength with group velocity, as shown in Table 1, one sees that the grid points G per wavelength of Q_1- and P_1 NC elements are required nearly twice to three times those of DSSY NC element depending on the wave propagation direction.

In the three-dimensional case, we set

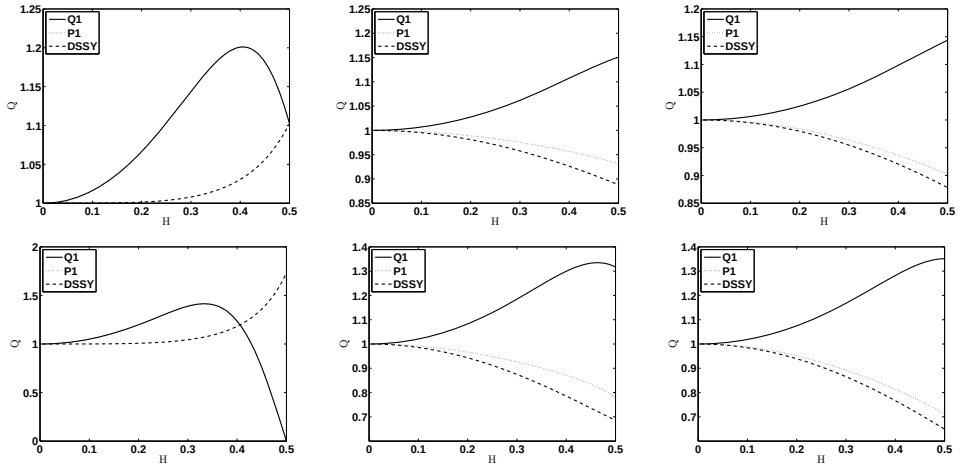

(a) $\theta = \varphi = 0$ (b) $\theta = \varphi = \pi/6$ (c) $\theta = \varphi = \pi/4$

Fig. 6. Phase and group velocities for the three-dimensional problem. H in x-axis means the reciprocal of the number of grid points, and the values on y-axis are the phase and group velocities according to the propagation direction $\theta = 0$, $\pi/6$, $\pi/4$.

$$\mathbf{k}^h = (k_1^h,\, k_2^h,\, k_3^h) = k^h(\cos\varphi\cos\theta,\, \cos\varphi\sin\theta,\, \sin\varphi),$$

where θ represents the angle measured from the positive x_1-axis to the vector $(k_1,\, k_2,\, 0)$ and φ the angle measured from the vector $(k_1,\, k_2,\, 0)$ to the vector $\mathbf{k}^h$. Fig. 6 shows the relation of phase velocity q and the number of grid points G with the propagation directions $\theta = \varphi = 0$, $\pi/6$, and $\pi/4$. From Fig. 6, we observe that among the three simplest finite elements the P_1 NC element requires the least number of grid points per wavelength to achieve the accuracy we want at several wave propagation directions. We remark that this is different from the case of two dimension. Table 2 shows the grid points G per wavelength to have the errors in group velocities within 1%. We compute G with the direction $\theta = \varphi = 0$, $\pi/6$, and $\pi/4$. In contrast to the two dimensional case, we realize that the use of P_1 NC element requires less number of grids per wavelength than the other two elements except for the case $\theta = \varphi = 0$.

wave direction($\theta = \varphi$)	Q_1 element	P_1 NC element	DSSY NC element
0	22.2	22.2	4.6
$\pi/6$	14.3	9.2	12.1
$\pi/4$	13.6	11.1	12.4

Table 2. The grid points G per wavelength to have the error within 1% in the three-dimensional case.

5.2. Comparison of relative errors according the degrees of freedom

To investigate the behavior of wave number, we choose the computational domain to be $\Omega = [0, 1]^2$ or $[0, 1]^3$ depending on its dimension and the source function f to be zero in (2.7) by taking a non-homogeneous boundary condition [1, 20]. The following relative error norms are then used:

$$E^0 := \frac{||u - u_h||_{0,h}}{||u||_{0,h}}, \qquad E^1 := \frac{|u - u_h|_{1,h}}{|u|_{1,h}},$$

where

$$||u||_{0,h} = \Big(\sum_j ||u||^2_{0,\Omega_j}\Big)^{1/2}, \quad |u|_{1,h} = \Big(\sum_j |u|^2_{1,\Omega_j}\Big)^{1/2}.$$

Given tolerance ϵ, let DOF(ϵ) denote the least degrees of freedom with which the error is less than or equal to the desired tolerance in the numerical experiments. For standard elliptic problem, the logarithm of DOF(ϵ) increases with constant speed as ϵ decreases regardless of using conforming or nonconforming elements. For Helmholtz type of problems this is not the case any more. Due to the pollution effect, *i.e.*, the non-robust behavior with respect to the wave number, the logarithm of DOF(ϵ) does not grow in constant speed any more and it may tend to infinity although ϵ is quite small [1, 3, 4, 11].

We restrict ourselves to the case that the mesh size h satisfy $hk \leq \pi/4$ so that the grid points per wave length are at least 8. To investigate comparing the errors with respect to the degrees of freedom, we fix the wave number k and vary the mesh size h. Due to the result of Cummings and Feng [2] on the elliptic regularity estimate for the Helmholtz equation in terms of k, one can easily modify the result of [3] on the $L^2(\Omega)$-error estimate such that there exists a positive constants K_0 such that

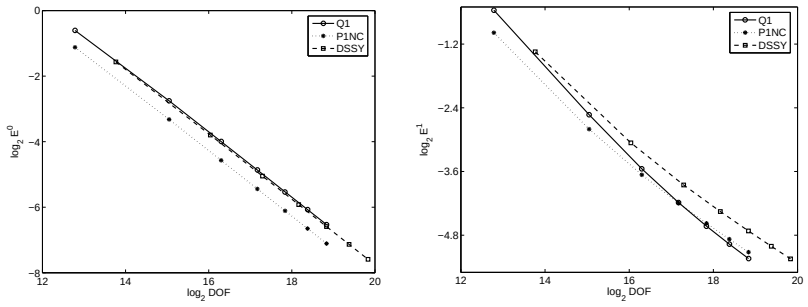

(a) $\theta = \pi/8$ (b) $\theta = \pi/8$

Fig. 7. E^0 and E^1 according the degrees of freedom for wave number k for the two-dimensional problem

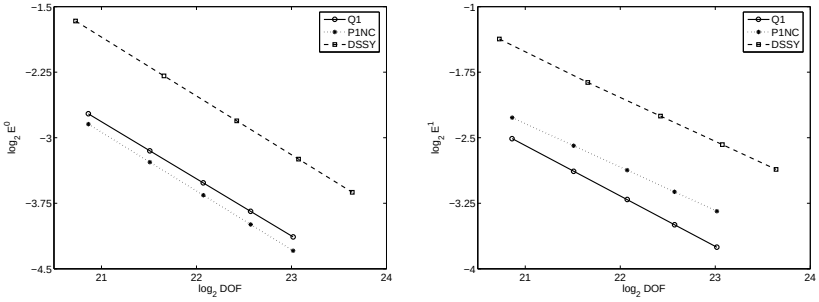

(a) $\theta = \pi/4$ and $\varphi = \pi/6$ (b) $\theta = \pi/4$ and $\varphi = \pi/6$

Fig. 8. E^0 and E^1 according the degrees of freedom for wave number k for the three-dimensional problem

$$\|u - u_h\|_0 \leq K_0(1+k)h^2\|f\| \quad \text{for large } k. \tag{5.2}$$

(5.2) implies that as the frequency becomes larger, the error grows at most linearly in k.

Fig. 7 shows the log-log plots of the E^0 and E^1 norms for $k = 65$ with the propagation direction for our two-dimensional problem. For the three-dimensional problem, Fig. 8 shows the log-log plots of E^0 and E^1 for $k = 65$.

Since $E^0 \le C_1(k,\, f)h^2$ and $E^1 \le C_2(k,\, f)h$, we have

$$\log E^0 \le \log C_1 + 2\log h, \quad \log E^1 \le \log C_2 + \log h, \tag{5.3}$$

where the constants C_1 and C_2 depend not on the mesh size h but on the frequency ω, the source function, and the finite elements. If the step size h is sufficiently small, the log-log plots for the relative errors show the slopes 2 and 1. We observe that regardless of its dimension, the error E^0 using P_1 NC element is smallest among those using the three elements. However, concerning the error E^1, the Q_1 conforming element shows the best performance when the mesh size is sufficiently small.

6. Conclusion

In this paper, we investigated in several features of using the P_1 NC element in solving two or three dimensional Helmholtz problems. Numerical dispersion analysis was carried out. Since the P_1 NC element is linear, the behavior is very similar to that of Q_1 conforming element. On the other hand, since the P_1 NC element is nonconforming, it reflects a similar property as the DSSY NC finite element. A primary benefit for using the P_1 NC element is of course that it requires less DOF(ϵ) than the other Q_1 conforming and DSSY NC elements within 1 % dispersion error in three-dimensional space. In case the wave number k increases under the same number of elements, for two-dimensional problems, the P_1 NC element is more sensitive to the wave number than the DSSY NC element. However, for three-dimensional problems, the P_1 NC element is less sensitive to the wave number than the other two Q_1 conforming and DSSY NC elements.

Acknowledgment This work was supported by the Korea Research Foundation (KRF-2006-070-C00014), KOSEF R01-2005-000-11257-0, and the Seoul R&BD Program. The work of Ha was supported by the National Institute of Mathematical Sciences(NIMS).

References

[1] Babuška I., Ihlenburg F., Paik E. and Sauter S., *A generalized finite element method for solving the Helmholtz equation in two dimensions with minimal pollution.* Comput. Methods Appl. Mech. Engrg. **128** (1995), 325–359.

[2] Cummings P. and Feng X., *Sharp regularity coefficient estimates for complex-valued acoustic and elastic Helmholtz equations*. Math. Models Methods Appl. Sci. (1) **16** (2006), 139–160.

[3] Douglas J. Jr., Santos J.E. and Sheen D., *Approximation of scalar waves in the space-frequency domain*. Math. Models Methods Appl. Sci. (4) **4** (1994), 509–531.

[4] Douglas J. Jr., Santos J.E., Sheen D. and Bennethum Lynn S., *Frequency domain treatment of one-dimensional scalar waves*. Math. Models Methods Appl. Sci. (2) **3** (1993), 171–194.

[5] Douglas J. Jr., Santos J.E., Sheen D. and Ye X., *Nonconforming Galerkin methods based on quadrilateral elements for second order elliptic problems*. ESAIM-Math. Model. Numer. Anal. (4) **33** (1999), 747–770.

[6] Feng X. and Sheen D., *An elliptic regularity estimate for a problem arising from the frequency domain treatment of waves*. Trans. Amer. Math. Soc. (2) **346** (1994), 475–487.

[7] Ha T., Lee H., Park C. and Sheen D., *The P_1-nonconforming hexahedral finite element*. 2007, in preparation.

[8] Harari I., *A survey of finite element methods for time-harmonic acoustics*. Comput. Methods Appl. Mech. Engrg. **195** (2006), 1594–1607.

[9] Honsberger R., *Episodes in nineteenth and twentieth century Euclidean geometry*. New Mathematical Library, vol. 37, The Mathematical Association of America, Washington, 1995.

[10] Ihlenburg F., *Fininte element analysis of acoustic scattering*. Applied Mathematical Sciences, vol. 132, Springer-Verlag, New York, 1998.

[11] Ihlenburg F. and Babuška I., *Dispersion analysis and error estimation of Galerkin fininte element methods for Helmholtz equation*. Int. J. Numer. Meth. Engng. **38** (1995), 3745–3774.

[12] Ihlenburg F. and Babuška I., *Finite element solution of the Helmholtz equation with high wave number*. I *The h-version of the FEM*. Comput. Math. Appl. (9) **30** (1995), 9–37.

[13] Mullen R. and Belytschko T., *Dispersion analysis of finite element semidiscretizations of the two-dimensional wave equation*. Internat. J. Numer. Methods Engrg. (1) **18** (1982), 11–29.

[14] Park C. and Sheen D., *P_1-nonconforming quadrilateral finite element methods for seond-order elliptic problems*. SIAM J. Numer. Anal. (2) **41** (2003), 624–640.

[15] Rannacher R. and Turek S., *Simple nonconforming quadrilateral Stokes element*. Numer. Methods Partial Differential Equations, **8** (1992), 97–111.

[16] Thompson L.L., *A review of finite element methods for time-harmonic acoustics*. J. Acoust. Soc. Amer. (3) **119** (2006), 1315–1330.

[17] Trefethen L.N., *Group velocity in finite difference schemes*. SIAM Rev. (2) **24** (1982), 113–136.

[18] Whitham G.B., *Linear and Nonlinear Waves*. John Wiley & Sons, New York, 1974.

[19] Zyserman F.I. and Gauzellino P.M., *Dispersion analysis of a nonconforming finite element method for the three-dimensional scalar and elastic wave equations*. Finite Elem. Anal. Des. **41** (2005), 1309–1326.

[20] Zyserman F.I., Gauzellino P.M. and Santos J.E., *Dispersion analysis of a nonconforming finite element method for the Helmholtz and elastodynamic equations*. Int. J. Numer. Meth. Engng. **58** (2003), 1381–1395.

T. Ha
National Institute for Mathematical Sciences
3F TowerKoreana 385-16
Doryong-dong, Yuseong-gu
Daejeon 305-340, South Korea
E-mail: tha@nims.re.kr

K. Lee
Office of Strategy Consulting
Samsung SDS
Seoul 135-918, Korea
E-mail: kitak.lee@samsung.com

D. Sheen
Department of Mathematics and Interdisciplinary Program in Computational Science & Technology
Seoul National University
Seoul 151-747, Korea

also currently visiting:
Department of Mathematics
Purdue University
West Lafayette
IN 47907, USA.
E-mail: sheen@snu.ac.kr